

Finite element modelling of two-way RC slabs with varying modelling choices

Jiangpeng Shu¹, David Fall¹, Mario Plos¹, Kamyab Zandi^{1,2}, Karin Lundgren¹

¹*Department of Civil and Environmental Engineering,
Chalmers University of Technology,
412 96 Gothenburg, Sweden*

²*Material Group,
CBI Swedish Cement and Concrete Research Institute,
501 15 Borås, Sweden*

Abstract

Non-linear finite-element (FE) method is today commonly used to simulate the behavior of reinforced concrete structures. The study presented in this paper comprises non-linear FE analyses of the behavior of two-way RC slabs and a comparison with experimental results. In the analyses, the concrete in compression was described by an isotropic damage constitutive law. In tension, a total strain model with rotating crack was adopted. The reinforcement was described by a Von Mises plasticity model, including hardening. The load-displacement relationship, and crack pattern of the two-way slabs under a concentrated load were compared to experimental results. The influence of some modelling choices, such as element type, mesh density, and reinforcement-concrete interaction were investigated. Analyses with varying mesh size resulted in very small difference in the results. The analysis including bond-slip gave lower stiffness at the cracking stage, and displayed more localized cracks compared to the analysis with full interaction, while both had the same ultimate load capacity.

1 Introduction

The non-linear behavior of reinforced concrete (RC) structural systems is complex because of the interaction between concrete and reinforcement and nonlinearity in material as well as in geometry. To accurately describe the nonlinear behavior of RC slabs, finite element (FE) methods have been investigated since early 1970s [1]. For a reliable FE analysis of RC slabs, efficient and robust numerical models are essential to accurately predict the structural behavior.

Two techniques exist for modeling RC structures regarding the interaction between concrete and reinforcement: full interaction and discrete modeling. In the first case, stiffness is added to concrete elements along the reinforcement while in the second case, the concrete and reinforcement are modeled separately with interface elements between them. Models for numerical simulation of concrete cracking are traditionally based on either the smeared crack model or the discrete crack model [2]. In the smeared crack model, the crack is modeled by modifying the strength and stiffness of concrete and by distributing or “smearing” the dissipated energy of a crack along the finite width of a localization band [3]. This, so called crack band approach [4], is widely adopted as a simple technique eliminating or reducing the sensitivity of numerical results to the mesh size of finite elements in simulations that involve strain localization due to softening. The present study was carried out to investigate and compare the efficiency and accuracy of different modeling choices, using the crack band approach in 3D finite element analyses of RC slabs. Tests carried out in the laboratory of Structural Engineering at Chalmers University of Technology were used for comparison.

2 Experiments of slabs

In a larger test series [5][6], three specimens containing traditional reinforcement alone were tested. The three specimens were intended to be equal; thus they had the same dimensions and reinforcement arrangements, and the results in the three tests were very similar. The specimens were two-way octagonal slabs (80 mm in thickness) supported on four edges, each by five rollers, and subjected to a point-load at the center, see Fig. 1. Moreover, the loading jack was coupled to a load cell which was placed over a steel plate (280 × 280 × 30 mm). Even load distribution was ensured by placing a wood fibre board ($t = 12$ mm) between the steel plate and the slab.

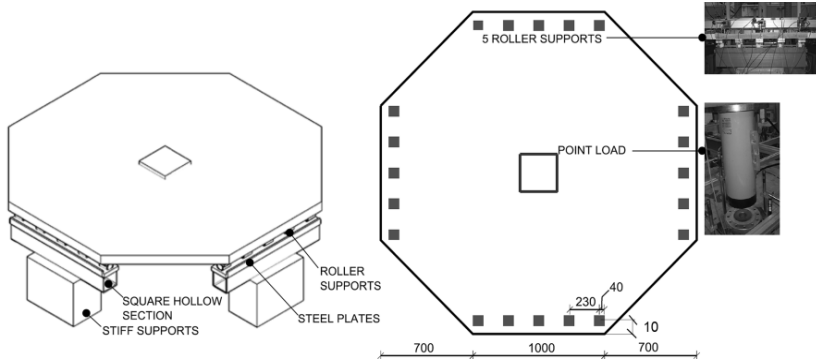


Fig. 1 Test set up of two-way slabs; all dimensions in mm

Twenty eight linear variable differential transformers (LVDTs) were used to measure the deformation of the slab's upper surface relative to the floor, see Fig. 2. The hydraulic jack was controlled by the LVDT designated as No. 25 in Fig. 2. Lastly, to adequately document the formation of the crack pattern under the large scale specimen, five video cameras were placed under the slab.

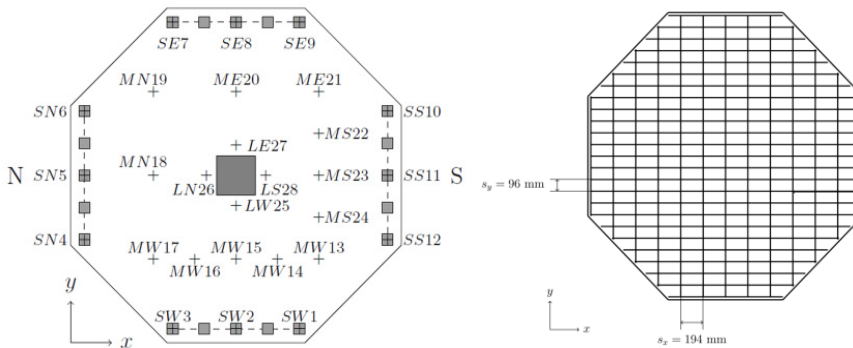


Fig. 2 LVDT instrumentation (left) and reinforcement layout (right)

Regarding the material, the compressive strength ($f_c = 50.9$ MPa) and tensile strength ($f_t = 2.7$ MPa) of the concrete, together with the tensile strength of steel reinforcement ($f_y = 621$ MPa, $E_s = 210$ GPa) were tested. The reinforcement had a bar diameter of 6 mm, placed with a clear cover of 20 mm from the bottom of the slab to the most dense layer; the layout is shown in Fig. 2.

3 Numerical models

3.1 Finite element model and numerical procedure

The finite element software DIANA 9.4.4 was used to model the slab, using a 3D model. Due to symmetry, only a quarter of the slab was included in the model, to reduce the computation time, Fig. 3. In the test, steel plates and roller bearings were used at the supports. In the FE model, the steel plates were modeled and interface elements were used between the concrete and the steel plates to count for friction. Under the steel plates at the supports, the nodes were supported in both vertical direction and along the roller supports. All nodes at the symmetry faces were fixed in the perpendicular direction.

In a phased analysis, the self-weight was first applied. Thereafter, the point load was applied as a prescribed vertical displacement to the center node at the top of the steel plate. Each step was equivalent to a vertical displacement of 0.1 mm until the deflection was 3 mm. For larger mid span deflections, the step size was increased to 1 mm to save computation time. Newton-Raphson iterative scheme was used to solve the non-linear equilibrium equations.

The response of the interface elements (between the concrete and the steel plates at the supports) was based on the Mohr-Coulomb criterion with tension cut-off. With this model, only compression is allowed. All parameters of the model used in the interface elements are presented in Table 1.

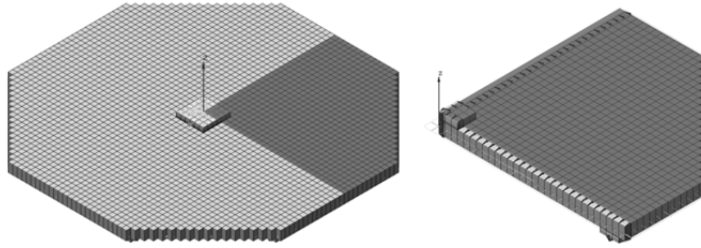


Fig. 3 FE model of the tested slabs

Table 1 Parameters of interface element

| | |
|--|----------------------|
| Normal stiffness [N/m ³] | 1.0×10^{13} |
| Tangential stiffness [N/m ³] | 1.0×10^{12} |
| Cohesion [MPa] | 1.0 |
| Friction angle | 15° |

To investigate the influence of variable modeling choices, several models with different element types, mesh density and ways to model the interaction between concrete and reinforcement were analyzed. The properties of the models are shown in Table 2. An analysis (analysis I) with 40 mm brick elements and full interaction to the reinforcement was selected as reference. In analysis II, wedge elements were chosen to investigate the influence of element types. In analyses III and IV, element sizes of 30, and 20 mm in plane were chosen, respectively, to study the influence of mesh density. In analysis V, a bond-slip relation was assumed for the interaction between reinforcement and concrete. Over the thickness of the slab, 8 layers of elements (each 10 mm) were chosen, independently of the in-plane element size, to describe bending behavior without costing too much computation time. It should be noted, that as the in-plane element size was varied while the element height was not, i.e. the aspect ratio of the elements varied between different element sizes.

Table 2 Five analyses with varying modeling choices

| Analyses | Element type | ES (element size) | Bond model |
|------------------------|---------------|-------------------|------------------|
| Analysis I (reference) | Brick element | 40 mm | Full interaction |
| Analysis II | Wedge element | 40 mm | Full interaction |
| Analysis III | Brick element | 30mm, | Full interaction |
| Analysis IV | Brick element | 20 mm | Full interaction |
| Analysis V | Brick element | 40 mm | Bond-slip |

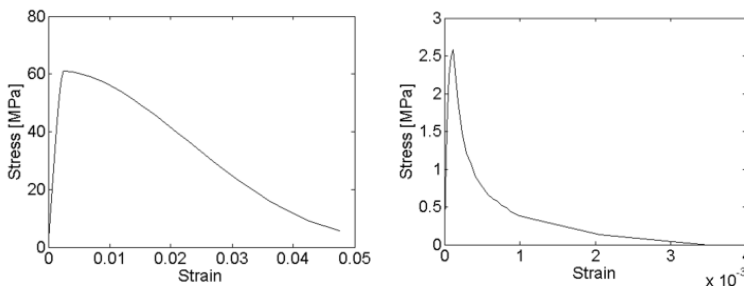


Fig. 4 Input for compressive (left) and tensile (right) models of concrete

3.2 Modeling of concrete

The concrete was modeled with a total strain rotating crack model [7]. The crack band width was assumed to be equal to the element size. The behavior of concrete in tension was taken from uniaxial

tension tests [8]. The behavior of concrete in compression was described by an isotropic damage constitutive law, and the stress-strain curve according to Thorenfeldt [9] was modified for the concrete element size as suggested in [10]. The material properties are shown in Fig. 4.

3.3 Modelling of reinforcement and concrete-reinforcement interaction

The reinforcement was described by a Von Mises plasticity model, including hardening, using values as obtained in material tests. The stress-strain relationship used is displayed in Fig. 5.

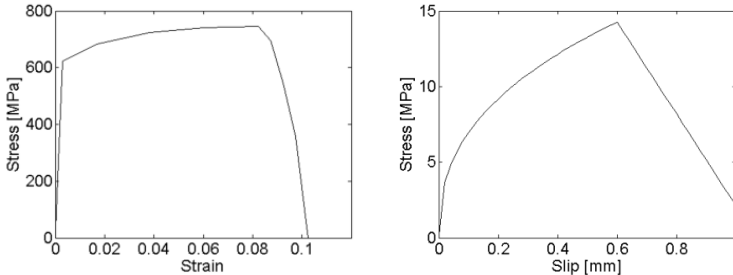


Fig. 5 Input for material model of reinforcement steel, and bond-slip model

In Analyses I to III, the reinforcement and concrete were assumed to be in full interaction; this is equivalent to that the reinforcement simply adds stiffness to the concrete element it is embedded in. In Analysis IV, the reinforcement bars were modelled as 2-noded truss elements, which were connected to the concrete elements by line interface elements. These interface elements described a bond-slip behavior in terms of a relation between the traction and the relative displacement. The analytical bond-slip relation for unconfined concrete under “good” bond conditions given in the CEB-FIP Model Code (1990) [11] was assumed for the concrete slab, Fig. 5. That is, $s_1 = s_2 = 0.6\text{mm}$, $\tau_{\max} = 14.26\text{MPa}$ and $\tau_f = 2.14\text{MPa}$.

4 Results and discussion

As mentioned, the three slabs tested showed similar results; here, the one with intermediate values (CR2) was taken as a reference to be compared with the analysis results. For this slab, cracking started when the load was around 30 kN, followed by bending hardening. The slab failed at an ultimate load of 71.4 kN.

4.1 Load-deflection

Comparing the results of the reference FE analysis with experimental (Fig. 6), the cracking load in the analysis was 34 kN, i.e. 13% higher than in the experiment. One reason is that in the analysis, cracking took place first when the tensile strength was reached in the bottom integration point of the slab; as this was situated 5 mm from the bottom, this means the crack was already 5 mm deep. In the analysis, the ultimate load was 56.7kN, 20% lower than that in the experiment. The failure in the analyses was defined when the analysis could not achieve convergence, which was always after reinforcement yielding.

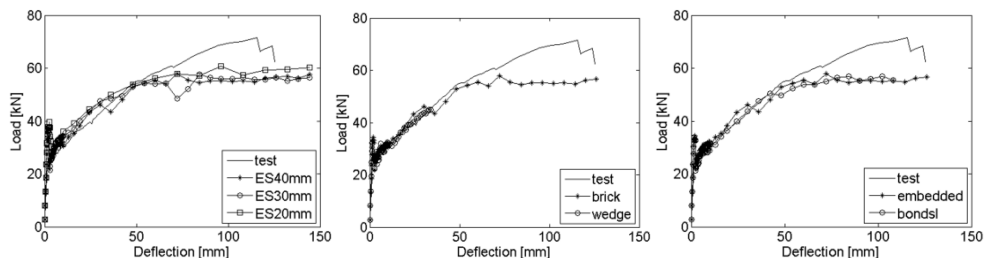


Fig. 6 Load versus mid-span deflection for different mesh densities (left), element types (middle) and bond models (right)

Comparing the models with different modeling choices, Fig. 6, the models with element size 40 mm and 30 mm showed similar results, while the model with 20 mm elements showed instability. With wedge elements, it was more difficult to achieve convergence than with brick elements; the analysis with wedge elements could not be continued further than a mid-span deflection of around 40 mm. The analysis with bond-slip interaction gave lower stiffness at the cracking stage but the same ultimate load capacity as the analysis with full interaction.

4.2 Crack pattern

Comparing the crack pattern of the reference FE analysis and experiment (Fig. 7), crack localization became more visible for decreasing element size (Column II). Concerning element shape, the cracks tended to propagate along the mesh direction (Column III); as wedge elements gave more freedom in this sense, the crack pattern in the analysis with wedge elements therefore agreed best with the experimental. The analysis including bond-slip displayed more localized cracks, while the model with full interaction showed distributed cracks (Column IV).

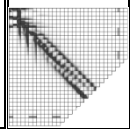
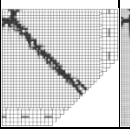
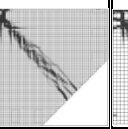
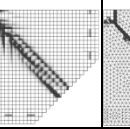
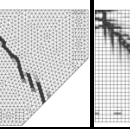
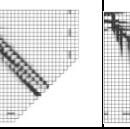
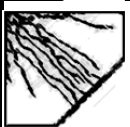
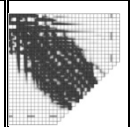
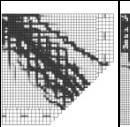
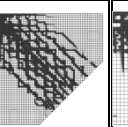
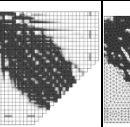
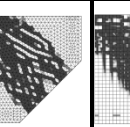
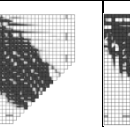
| Column I | Column II | | | Column III | | Column IV | |
|---|---|---|---|---|---|--|---|
| | Element Size | | | Element Type | | Bond model | |
| Experimental | 40mm <i>Analysis I</i> | 30mm <i>Analysis III</i> | 20mm <i>Analysis IV</i> | Brick <i>Analysis I</i> | Wedge <i>Analysis II</i> | Full interaction <i>Analysis I</i> | Bond-slip <i>Analysis V</i> |
|  |  |  |  |  |  |  |  |
|  |  |  |  |  |  |  |  |

Fig. 7 Crack pattern from the experiment (column I); and FE analysis with different element size (column II), with different element types (column III) and with different concrete-reinforcement interaction models (column IV) at initial crack state and at ultimate state

5 Conclusions

The study presented in this paper comprises non-linear FE analyses of the structural behavior of two-way RC slabs and a comparison with experimental results. The load-deflection relationship and crack pattern of the two-way slabs under concentrated load were compared to experimental results. The influence of some modeling choices, such as element types, mesh densities, and reinforcement-concrete interaction was investigated.

As cracks tend to propagate along the mesh shape, wedge would be preferred over brick elements; however, in this study, it was easier to reach convergence in the analyses with brick elements because it had better mesh quality. Analyses with varying mesh size resulted in very small difference in the results. The analysis including bond-slip gave lower stiffness at the cracking stage, and displayed more localized cracks compared to the analysis with full interaction, while both had the same ultimate load capacity.

Acknowledgment

The presented research was funded by the Swedish Transport Administration (Trafikverket) and the European Community's Seventh Framework Programme under grant agreement NMP2-LA-2009-228663 (TailorCrete). More information about the research project TailorCrete can be found at www.tailorcrete.com.

References

- [1] Jofriet C, McNiece M. Finite element analysis of reinforced concrete slabs. *J Struct Div, ASCE* 1971;785–806.
- [2] Plos M. Compendium 96:14 Finite element analyses of reinforced concrete structures. Gothenburg, Chalmers University of Technology; 2000.
- [3] Jirásek M, Bauer M. Numerical aspects of the crack band approach. *Comput Struct* 2012;110-111:60–78.
- [4] Bazant ZP, H OB. Crack band theory for fracture of concrete 1983.
- [5] Fall D, Shu J, Rempling R, Lundgren K, Zandi K. Two-way slabs : Experimental investigation of plastic redistributions in Steel Fibre Reinforced Concrete. *Eng Struct* 2014. (submitted)
- [6] Portal NW, Thrane L, Lundgren K. Flexural Behaviour of Textile Reinforced Concrete (TRC). *Cem Concr Compos* 2013. (submitted)
- [7] Jonna Manie. Diana User's Manual -- Release 9.4.4. TNO DIANA BV 2011.
- [8] Rempling R, Fall D, Lundgren K. Three point bending and uni-axial tension tests of double hook-end fibers. 7th Int. Conf. Fibre Concr. 2013., Prague, the Czech Republic: 2013.
- [9] Thorenfeldt, E., Tomaszewicz, A., and Jensen JJ. Mechanical properties of high-strength concrete and applications in design. *Proc. Symp. Util. High-Strength Concr.*, 1987.
- [10] Zandi K, Ketti P, Lundgren K. Modeling the Structural Behavior of Frost-damaged Reinforced Concrete Structures. *Struct Infrastruct Eng* 2010;9:416–31.
- [11] CEB-FIP model code 1990. Lausanne, Switzerland: 1993.